

## Ultrafast Optical Switching in Three-Dimensional Photonic Crystals

D. A. Mazurenko,\* R. Kerst, and J. I. Dijkhuis

*Atom Optics and Ultrafast Dynamics, Debye Institute, Department of Physics and Astronomy, University of Utrecht, P.O. Box 80000, 3508 TA Utrecht, The Netherlands*

A. V. Akimov, V. G. Golubev, D. A. Kurdyukov, A. B. Pevtsov, and A. V. Sel'kin

*Ioffe Physico-Technical Institute, Russian Academy of Sciences, St. Petersburg 194021, Russia*

(Received 14 March 2003; published 19 November 2003)

We present the first experimental investigation of ultrafast optical switching in a three-dimensional photonic crystal made of a Si-opal composite. Ultrafast (30 fs) changes in reflectivity around the photonic stop band up to 1% were measured for moderate pump power ( $70 \mu\text{J}/\text{cm}^2$ ). Short-lived photoexcited carriers in silicon induce changes in the dielectric constant of Si and diminish the constructive interference inside the photonic crystal. The results are analyzed within a model based on a two-band mixing formalism.

DOI: 10.1103/PhysRevLett.91.213903

PACS numbers: 42.70.Qs, 42.65.Sf, 42.79.Ta, 78.47.+p

Three-dimensional (3D) photonic crystals are materials with a periodically modulated index of refraction on the scale of the wavelength of light, and can be used to realize a complete photonic band gap and as a basis for new photonic devices [1–4]. This leads to an interest in the ultrafast, nonlinear optical properties of such materials. As has been predicted recently [5,6], the 3D photonic crystal must be switchable on a femtosecond time scale by hot carriers generated in a semiconductor. Recently, ultrafast switching has been realized in 1D [7] and 2D [8] Si-based photonic crystals. Experimental switching in 3D photonic crystals was studied on the nanosecond time scale [9,10].

Here, we present the first experimental results of femtosecond pump-probe experiments in a 3D photonic crystal in the region of the photonic stop band (PSB). To demonstrate the ultrafast optical switching we chose Si-embedded opals: opals are known to be the model objects in studying PSB effects [11,12], and silicon is very suitable for a dynamic experiment, because of its weak but noticeable absorption in the near-infrared region, its high index of refraction, and its short carrier lifetime. Moreover, Si-opal structures can be integrated in optical circuits [2].

Our sample is composed of close-packed 230-nm diameter  $\text{SiO}_2$  spheres forming an ordered fcc polydomain opalescent matrix. The filling factor of silicon in opal voids was close to 100%. The first-order PSB of the sample is localized around 800 nm. The scanning electron microscopy [13] studies showed that the size of a single domain ranges from 30 to 100  $\mu\text{m}$ . The sample was cut out in a 0.5-mm thick plate, with the surface (area of 10  $\text{mm}^2$ ) almost parallel to the (111) surface. Further details of growth and optical properties of the sample can be found in Ref. [13]. The stationary reflectance spectra were measured with a halogen lamp, a spectrometer, and a charge-coupled device. The collimated 2-mm diameter beam from the lamp was sent along the same optical path

as a probe laser beam (Fig. 1). The difference in the propagation direction of the Bragg-diffracted beam and the specular beam allowed us to distinguish the effects from the 3D opal structure and the ordinary surface reflection of the sample. In the first configuration the specular beam was blocked, and only the Bragg-diffracted light was collected over a solid angle of  $3.5 \times 10^{-2}\pi$ . In the second configuration a diaphragm of 2-mm diameter selected the specular beam and suppressed the Bragg light. Because of structural defects in the opal lattice [14–17] the Bragg light emerges as a cone extending over several degrees depending on the point selected at the sample surface.

In Fig. 2 the symbols show the measured stationary reflectance spectra for the two configurations. The Bragg-diffracted spectrum  $R_d$  peaks around  $\lambda = 790 \text{ nm}$  and has a width of 66 nm, in agreement with earlier studies of

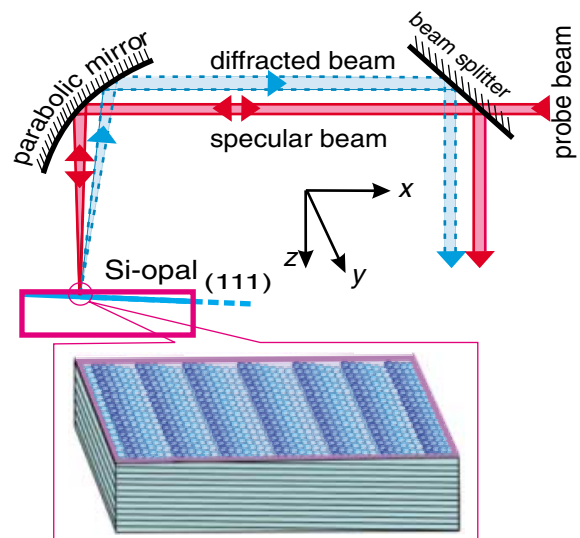


FIG. 1 (color online). Diagram illustrating the beam paths of the incident probe, the specular, and the Bragg diffracted beams. Inset schematically shows the faceted sample surface.

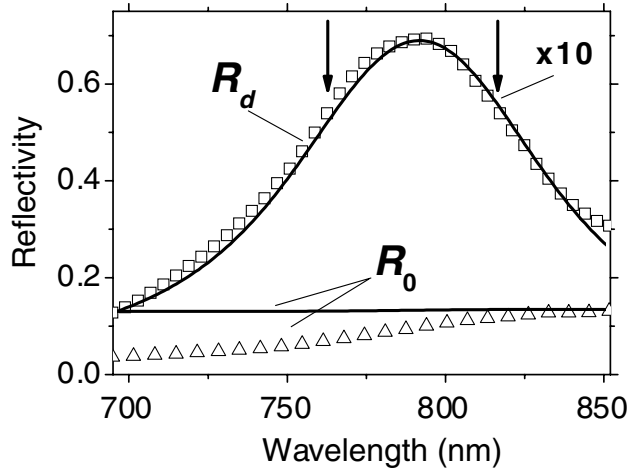


FIG. 2. Measured (symbols) and calculated (solid lines) spectra of specular reflection ( $R_0$ ) and Bragg diffraction efficiency ( $R_d$ ). Experimental data are normalized to the maximum of the  $R_d$  theoretical curve. Vertical arrows point the calculated positions of the photonic band edges when the imaginary part of dielectric constants is neglected.

similar samples. The origin of the peak is attributed to the PSB [13]. The specularly reflected light  $R_0$  has a higher intensity, but does not exhibit the PSB structure.

The transient reflectivity was measured using a special setup that suppresses interference during the temporal overlap between the pump and probe pulses. The beam from a 15-fs Ti-sapphire laser (FEMTOSOURCE) with a repetition rate of 75 MHz was split by a standing wave acousto-optic modulator (AOM) operating at 35.5 MHz. Thus the first-order diffracted beam, acting as the probe, was strongly phase modulated relative to the zero-order (nondiffracted) beam, acting as the pump. The pump and the probe beams were made cross polarized, which further suppresses interference. To compensate for the chirp induced by the AOM crystal, both pump and probe beams were reflected 16 times from mirrors with a negative dispersion, leading to an overall 30-fs time resolution. The parallel probe beam was passed via a computer-controlled delay line with 1- $\mu\text{m}$  precision. The pump and probe beams (4 and 2 mm diameter, respectively) were focused on the same 85- $\mu\text{m}$  spot at the sample surface at a near-zero angle of incidence using a parabolic mirror. The surface energy densities of the probe and pump pulse on the surface were 5 and 70  $\mu\text{J}/\text{cm}^2$ , respectively. The reflected probe light was picked up by a beam splitter, passed through the spatial filter, and focused on a photodiode. Scattered pump light was rejected by a polarizer. The absolute nonlinear changes in the reflected probe intensity  $\Delta R(t)/R$  were extracted by standard double modulation techniques and a calibrated lock-in amplifier operated at the sum frequency ( $\sim 1$  kHz).

Typical pump-probe signals are presented in Fig. 3 for the specular [ $\Delta R_0(t)/R_0$ , dashed line] and Bragg-

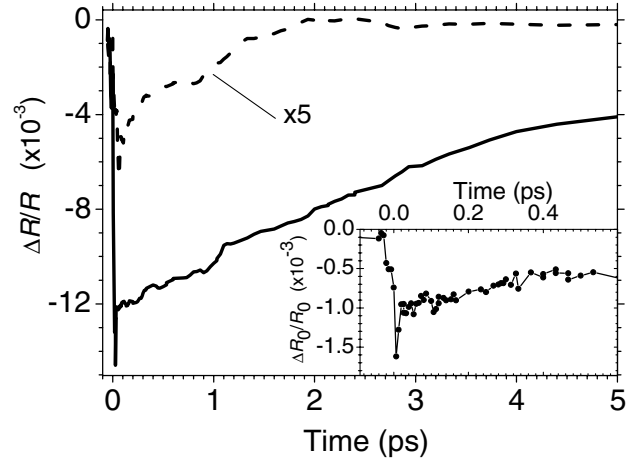


FIG. 3. Temporal evolutions of transient changes in specular reflection (dashed line) and Bragg diffraction efficiency (solid line). Inset shows the signal measured with 30 fs time resolution.

diffracted case [ $\Delta R_d(t)/R_d$ , solid line]. The inset of Fig. 3 displays an expanded time trace of  $\Delta R_0(t)/R_0$ . Both signals exhibit switching in less than 30 fs, limited by the time resolution of our experiment. The subsequent decay is multiexponential with time constants  $\tau_1 \sim 0.5 \pm 0.2$  ps and  $\tau_2 \sim 5 \pm 2$  ps. We note that the measured time constants vary over the sample surface by no more than 50%.

The most important experimental result is the large difference between the relative amplitudes of the transient signals,  $\Delta R_d(t)/R_d = -(1.2 \pm 0.2) \times 10^{-2}$  and  $\Delta R_0(t)/R_0 = -(9 \pm 2) \times 10^{-4}$ . This effect, observed for all points studied at the sample surface, leads us to the conclusion that pump light induces large ultrafast changes in PSB properties of our 3D Si-opal photonic crystal. Evidently, these pump-induced changes in the optical properties of the photonic crystal should depend on the pump-probe wavelength. For this reason, we carried out experiments in the PSB spectral range with a tunable 170-fs Ti-sapphire laser (MIRA) using the same setup but without a spatial filter. The dependence of the amplitude of the obtained transient signal  $\Delta(R_0 + R_d)/(R_0 + R_d)$  on the pump-probe wavelength is shown in Fig. 4 as symbols. Unfortunately, the high noise level of the intensity of this laser introduces quite sizable errors. However, in the spectral region which was available in the laser tuning range we clearly observed that the photoinduced signal is not constant but rises upon entering the PSB.

The measured temporal evolution of  $\Delta R(t)$  (Fig. 3) has a complicated shape. The pronounced peak around zero time delay is the contribution from instantaneous Kerr effect [18]. The subsequent evolution of  $\Delta R(t)$  is controlled by photoexcited electrons and holes in silicon. The presence of free carriers changes the complex dielectric constant of Si,  $\epsilon_{\text{Si}} = \epsilon'_{\text{Si}} + i\epsilon''_{\text{Si}}$ , that, in turn,

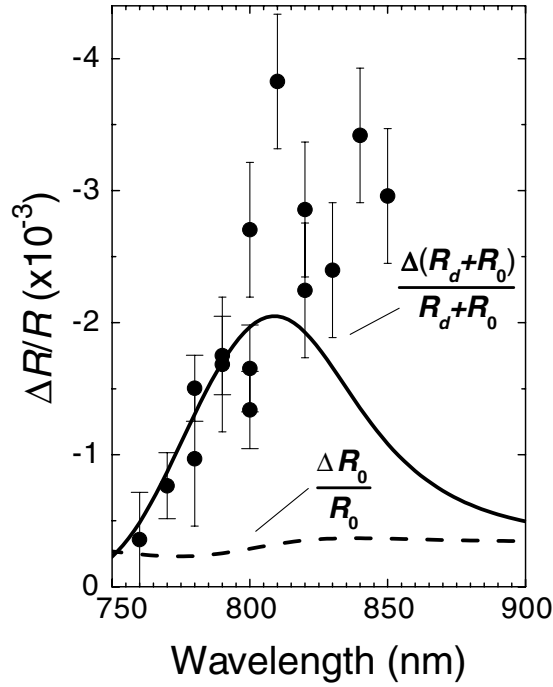


FIG. 4. Calculated (solid line) and measured (symbols) spectra of the photoinduced relative changes in the total reflection. Dashed line shows the calculated relative changes in the specular reflection.

changes the mean dielectric constant  $\bar{\epsilon}$  and, correspondingly, modifies the photonic density of states of the photonic crystal. The shape of  $\Delta R(t)$  (Fig. 3) is similar to the signals obtained in nanocrystalline Si films [19] and amorphous Si films [20,21] and was attributed to the energy relaxation of free carriers.

In order to explain the observed reflection and diffraction phenomena, we developed a quantitative model. The model is based on the two-band mixing formalism [22] that analyzes surface effects in photonic crystals and considers Bloch modes involving electromagnetic plane waves with only two wave vectors  $\mathbf{K}$  and  $\mathbf{K} - \mathbf{G}$ . Here,  $\mathbf{G}$  is the reciprocal-lattice vector for the [111] direction, with  $|\mathbf{G}| = 2\pi/L_{111}$  and  $L_{111}$  being a lattice period along the [111], and  $\mathbf{K}$  is the Bloch vector satisfying the condition  $(\mathbf{K} \cdot \mathbf{G}) \approx |\mathbf{G}|^2/2$  near the  $L$  point of the first Brillouin zone.

Only three terms survive in the dielectric function,

$$\epsilon(\mathbf{r}) \approx \bar{\epsilon} + \epsilon_{\mathbf{G}} e^{i\mathbf{G}\mathbf{r}} + \epsilon_{-\mathbf{G}} e^{-i\mathbf{G}\mathbf{r}}. \quad (1)$$

Here  $\bar{\epsilon} = \epsilon_{\text{Si}}(1-f) + \epsilon_s f + i\bar{\epsilon}''$ , with  $\epsilon_s$  the dielectric constant of  $\text{SiO}_2$  spheres,  $f = 0.74$  the relative volume of the pores filled with Si, and  $\bar{\epsilon}''$  the imaginary part of  $\bar{\epsilon}$  due to elastic light scattering at imperfections of the opal. Further,  $\epsilon_{\mathbf{G}}$  and  $\epsilon_{-\mathbf{G}}$  are the appropriate Fourier coefficients, which characterize the spatial modulation of  $\epsilon(\mathbf{r})$  along the [111] direction. It is clear that  $|\epsilon_{\mathbf{G}}| \propto |\text{Re}(\epsilon_{\text{Si}} - \epsilon_s)|$ . Solution of Maxwell's equations for

transverse electromagnetic waves yields the dispersion equation

$$\mathbf{n}^2 - \bar{\epsilon} = \frac{|\epsilon_{\mathbf{G}}|^2}{(\mathbf{n} - \mathbf{g})^2 - \bar{\epsilon}}, \quad (2)$$

where  $\mathbf{n} \equiv \mathbf{K}\lambda/2\pi$  and  $\mathbf{g} \equiv \mathbf{G}\lambda/2\pi$  with  $\lambda$  being the wavelength of light in vacuum.

We chose the  $z$  axis coincident with the inner normal to the surface of the photonic crystal (Fig. 1). Further,  $x$  and  $z$  define the plane of incidence and  $G_y = 0$ . Naturally, the tangential component of the incident wave vector is equal to that of the transmitted Bloch wave vector  $K_x$ , i.e.,  $n_x = \sin\theta$ , where  $\theta$  is the angle of incidence.

Equation (2) has four roots  $n_{jz}$  ( $j=1-4$ ) for the  $z$  component of the  $\mathbf{n}$  vector, each corresponding to a Bloch-mode electric field

$$\mathbf{E}_{\mathbf{K}}(\mathbf{r}) = \mathbf{A}_{\mathbf{K}} e^{i\mathbf{K}\mathbf{r}} \left[ 1 + \frac{\epsilon_{-\mathbf{G}}}{(\mathbf{n} - \mathbf{g})^2 - \bar{\epsilon}} e^{-i\mathbf{G}\mathbf{r}} \right], \quad (3)$$

where  $\mathbf{A}_{\mathbf{K}}$  is the coordinate-independent Bloch amplitude, but only roots with positive imaginary parts are physical. We are left with two  $y$ -polarized Bloch modes, with  $K_{1z}$  and  $K_{2z}$  at a given  $\theta$ .

Allowing for an incident small but nonzero tangential wave vector component on the surface, we use the Maxwellian boundary conditions for both zero and first-order diffraction. We arrive at a specular reflection coefficient  $R_0$  and nonspecular, diffracted reflection coefficient  $R_d$ ,

$$R_0 = \left| \frac{a-b}{a+b} \right|^2 \quad \text{and} \quad R_d = \left| \frac{d}{a+b} \right|^2, \quad (4)$$

with

$$a = (n_- + n_+)(n_- + n_+ + 1 - |\mathbf{g}|) - n_- n_+ - \bar{\epsilon},$$

$$b = (n_- n_+ + \bar{\epsilon})(1 - |\mathbf{g}|) + n_- n_+(n_- + n_+),$$

$$d = 2(n_-^2 - \bar{\epsilon})(n_+^2 - \bar{\epsilon})/\epsilon_{\mathbf{G}},$$

$$n_{-,+} = |\mathbf{g}|/2 + \sqrt{|\mathbf{g}|^2/4 + \bar{\epsilon} \pm \sqrt{|\mathbf{g}|^2 \bar{\epsilon} + |\epsilon_{\mathbf{G}}|^2}}.$$

The calculated spectra of  $R_d$  and  $R_0$  are indicated as solid lines in Fig. 2 for 227-nm diameter  $\text{SiO}_2$  spheres and  $\epsilon_s = 1.98$ . In the calculations values for  $|\epsilon_{\mathbf{G}}| = 0.308$ ,  $\epsilon_{\text{Si}}' = 12.25$ , and  $\bar{\epsilon}'' = 0.34$  were inserted. Further, the value for  $\epsilon_{\text{Si}}'' = 0.49$  was obtained from the absorption coefficient at 800 nm for Si grown at low annealing temperatures  $\alpha = 10^4 \text{ cm}^{-1}$  [23,24]. Both the central position and the width of  $R_d$  (Fig. 2) are satisfactorily reproduced. Only the calculated specular reflectance spectrum  $R_0$  deviates from the measured one and  $R_d$  does not show the experimentally observed background. The very general reason for these deviations, which turn out to vary over the sample, is the spectral dependence of the extinction due to various imperfections that causes light to be diffracted nonspecularly, grain boundaries

between crystal domains or transition layers that may exist at the surface.

Transient changes  $\Delta R_d$  and  $\Delta R_0$  may also be calculated from Eq. (4), given the photoinduced changes  $\Delta \epsilon_{\text{Si}} = \Delta \epsilon'_{\text{Si}} + i\Delta \epsilon''_{\text{Si}}$  in the dielectric constant of Si known from the Drude model [20]:

$$\Delta \epsilon'_{\text{Si}} = \frac{-Ne^2}{m^* \epsilon_0 (\omega^2 + \tau_d^{-2})} \quad \text{and} \quad \Delta \epsilon''_{\text{Si}} = \frac{-\Delta \epsilon'_{\text{Si}}}{\omega \tau_d}. \quad (5)$$

Here  $\epsilon_0$  is the permittivity of vacuum,  $m^* = 0.15m_0$  [25] the optical reduced mass,  $\tau_d = 0.5$  fs [26] the Drude damping time,  $\omega = 2.4 \times 10^{15}$  s<sup>-1</sup> the center frequency of the laser, and  $N = \alpha P_{\text{pump}}/\hbar\omega$  the density of photo-induced carriers. We obtain  $\Delta \epsilon_{\text{Si}} = (-6.2 + i5.3) \times 10^{-3}$  for our experimental conditions ( $P_{\text{pump}} = 70$   $\mu\text{J}/\text{cm}^2$ ).

Calculated Eq. (4) at 800 nm gives  $\Delta R_d/R_d = -5 \times 10^{-3}$  and  $\Delta R_0/R_0 = -3 \times 10^{-4}$ . Our calculation reproduces the more than 1 order-of-magnitude higher photo-induced changes in the Bragg reflectance spectra compared to the specular light ones.

The main cause for the strong transient Bragg signal is the high sensitivity of the photonic band structure in the opal to photoinduced changes in the dielectric constant of Si that fills the pores of the opal. The absolute calculated values for  $\Delta R_d/R_d$  and  $\Delta R_0/R_0$  at 800 nm deviate from the experimental values only by a factor of 2 and a factor of 3, respectively. We attribute this to a higher optical density of pump light in Si than assumed in the model, due to the field localization effects [27]. In Fig. 4 we show calculated (solid line) and measured (symbols) spectra of the relative changes in the total reflection  $\Delta R/R = \Delta(R_d + R_0)/(R_d + R_0)$ . The dashed line shows the calculated  $\Delta R_0/R_0$ . As we mention above, the experimental values of differential reflection are somewhat higher than the calculated in the region of PSB. Nevertheless, the calculated and measured values for various wavelengths of the photoinduced effects (Fig. 4) are in reasonable agreement. We finally note that the amplitude of the photoinduced changes of the Bragg diffraction intensity depends on the pump power density [26]. Although the amplitude of observed changes was low ( $\sim 1\%$ ), we believe that at higher power of the optical excitation the relative decrease of the photoinduced signal should reach as much as 50% or higher [8].

In conclusion, we have demonstrated ultrafast switching of PSB properties in a Si-opal composite. For relatively weak excitation pulses, we measured photoinduced changes for the Bragg diffraction intensity up to  $\sim 1\%$ , much higher than relative changes in the specular reflectance from the surface. Our results are in agreement with a theoretical model that properly takes into account surface effects and multiple scattering in the 3D photonic crystal. Our results show a way to control the photonic

band structure in 3D photonic crystal on a femtosecond time scale that is promising for a variety of interesting applications, such as switching of spontaneous emission.

We are grateful to C. R. de Kok, O. L. Muskens, and P. Jurrius for their technical assistance. This work was supported by the Russian Academy of Sciences and the RFBR. A.V.A. acknowledges financial support from the Netherlands Foundation ‘‘Fundamenteel Onderzoek der Materie’’ (FOM) and ‘‘Nederlandse Organisatie voor Wetenschappelijk Onderzoek’’ (NWO).

\*Electronic address: D.A.Mazurenko@phys.uu.nl

- [1] S. Y. Lin *et al.*, Nature (London) **394**, 251 (1998).
- [2] Y. A. Vlasov, X. Z. Bo, J. C. Sturm, and D. J. Norris, Nature (London) **414**, 289 (2001).
- [3] A. Blanco *et al.*, Nature (London) **405**, 437 (2000).
- [4] V. G. Golubev *et al.*, Appl. Phys. Lett. **79**, 2127 (2001).
- [5] P. M. Johnson, A. F. Koenderink, and W. L. Vos, Phys. Rev. B **66**, 081102(R) (2002).
- [6] Y. K. Ha *et al.*, Phys. Rev. B **66**, 075109 (2002).
- [7] A. Haché and M. Bourgeois, Appl. Phys. Lett. **77**, 4089 (2000).
- [8] S. W. Leonard, H. M. van Driel, J. Schilling, and R. Wehrspohn, Phys. Rev. B **66**, 161102(R) (2002).
- [9] G. Pan, R. Kesavamoorthy, and S. A. Asher, Phys. Rev. Lett. **78**, 3860 (1997).
- [10] A. V. Akimov *et al.*, Phys. Solid State **45**, 240 (2003).
- [11] T. F. Krauss and R. M. D. L. Rue, Prog. Quantum Electron. **23**, 51 (1999).
- [12] C. M. Soukoulis, *Photonic Crystals and Light Localization in the 21st Century*, Nato Advanced Studies Institute, Ser. C (Kluwer, Dordrecht, 2001), Vol. 653.
- [13] V. G. Golubev *et al.*, Semiconductors **35**, 680 (2001).
- [14] V. N. Astratov *et al.*, Phys. Rev. B **66**, 165215 (2002).
- [15] Y. A. Vlasov *et al.*, Phys. Rev. E **61**, 5784 (2000).
- [16] J. F. G. López and W. L. Vos, Phys. Rev. E **66**, 036616 (2002).
- [17] J. Huang *et al.*, Phys. Rev. Lett. **86**, 4815 (2001).
- [18] M. Sheik-Bahae, D. C. Hutchings, D. J. Hagan, and E. W. V. Stryland, IEEE J. Quantum Electron. **27**, 1296 (1991).
- [19] K. E. Myers, Q. Wang, and S. L. Dexheimer, Phys. Rev. B **64**, 161309(R) (2001).
- [20] A. Esser *et al.*, Phys. Rev. B **41**, 2879 (1990).
- [21] V. Klimov, D. McBranch, and V. Karavanskii, Phys. Rev. B **52**, R16989 (1995).
- [22] K. W. K. Shung and Y. C. Tsai, Phys. Rev. B **48**, 11265 (1993).
- [23] H. Richter and L. Ley, J. Appl. Phys. **52**, 7281 (1981).
- [24] Y. He *et al.*, J. Appl. Phys. **75**, 797 (1994).
- [25] K. Sokolowski-Tinten and D. von der Linde, Phys. Rev. B **61**, 2643 (2000), and Ref. [48] therein.
- [26] A. Esser *et al.*, J. Appl. Phys. **73**, 1235 (1993).
- [27] N. A. R. Bhat and J. E. Sipe, Phys. Rev. E **64**, 056604 (2001).